UNIVERSITY of CALIFORNIA
SANTA CRUZ

THERMAL EVOLUTION OF URANUS AND NEPTUNE WITH CONDENSATION-INHIBITED CONVECTION

A thesis submitted in partial satisfaction of the
requirements for the degree of

BACHELOR OF SCIENCE

in

ASTROPHYSICS

by

Robert Schroder

November 2020

Abstract

Thermal Evolution of Uranus and Neptune with Condensation-inhibited Convection

by

Robert Schroder

This will be the last section written, once we have finished our results and conclusion.

Contents

List of Figures

List of Tables

To Who,

M ention to who, if anyone, here

Acknowledgements

I'd like to think....

1

Introduction

Giant planets radiate away their latent heat of formation through the top of their atmosphere. If they cool to a point where the amount they radiate away is equal to the amount of radiation they receive from their parent star, they enter thermal equilibrium with their surroundings. At the present time, the giant planets in our solar system, Saturn, Jupiter, Uranus, and Neptune, all have effective temperatures greater than their equilibrium temperature, except for Uranus. Observations of Uranus show a planet that appears to be in thermal equilibrium with its parent star, a 'dead' planet with no intrinsic temperature, cooler than its more distant neighbor, Neptune. Thermal evolution models for Uranus have not matched observation, instead predicting a warmer effective temperature during the current epoch(Fortney et al., 2011), (M. Podolak, 1991), (W.B. Hubbard, 1995), (L. Scheibe, 2019) [There are other papers by Nettelmann 2013, Linder 2019 that I haven't looked at yet].

There have been various attempts to explain the cool Uranus. [The remainder of this paragraph is poorly worded] One of the first explanations posited a stratified interior, possibly stable against convection, that would allow heat deep to be trapped within the the interior.(M. Podolak, 1991). Later work has investigated the formation of stable condensation zones, composed of water, methane, or ammonia, that would inhibit convection (Friedson & Gonzales, 2017), (Leconte et al., 2017), and (Guillot, 1995). The presence of these condensation zones could trap heat deep within the interior, allowing the temperature in the envelope above the zone to cool more rapidly, lowering the planet's effective temperature.

The purpose of this paper is to examine.... We use the model described in chapter 2.1 as our comparison... The specifics of our model is described in chapter 2.2.

2

Model

2.1 Background: Interior Structure with Dry Convection

Understanding the physics of solar system gas and ice giant planets, and attempts to model their thermal evolution date back to the mid to late twentieth century (Hubbard, 1977b), (Hubbard, 1977a), and (M. Podolak, 1991). The description of the planetary interiror begins with the following equations. Conservation of mass:

$$\frac{dm}{dr} = 4\pi r^2 \rho \tag{2.1}$$

where dm is the mass contained within a sphere of radius r. $\rho(r)$ is the density at radius r. Hydrostatic equilibrium is assumed and described by:

$$\frac{dP}{dr} = -\frac{Gm\rho}{r^2} \tag{2.2}$$

where P is the pressure and G is the gravitational constant.

[include thermal evolution and conservation of energy discussion here]

$$\frac{dL}{dm} = -T\frac{\delta s}{\delta t}. \tag{2.3}$$

Integrating over the mass of the planet and solving for the timestep, δt, yields

$$\delta t = -\frac{1}{L_{\text{int}}}\int_0^M T\,\delta s\,dm \tag{2.4}$$

where L_{int} is the intrinsic luminosity, given by:

$$L_{\text{int}} = 4\pi r^2 \sigma_{\text{SB}} T_{\text{int}}^4 \tag{2.5}$$

A common practice is to assume a three-layer interior structure (CITE), which we assume for our model as well, as seen in Figure 2.1. At the center of the planet is a core made of ??. The inner envelope is H_2O dominated, with uniform concentrations of H, He, and H_2O, using the MAZEVET EOS (S. Mazevet & Potekhin, 2019). The outer envelope, below 10 bars, contains trace amounts of H_2O, but is mostly H and He, dominated, and utilizes the MH13SCVH EOS (Y. Miguel & Fayon, 2018).

Historically, interior structure models have assumed that the interiors are composed of compressible gasses that are statically unstable and fully convective. In a dry-convective model such as this, a parcel of gas rises as its temperature increases while its pressure remains constant. This process happens without the addition or loss of heat from the parcel, a process referred to as adiabatic. Furthermore, while there may be a critical concentration for a condensible species, all this dry model does not allow for condensation. The temperature-pressure profile follows a dry adiabat gradient(R. Kippenhahn, 2012), given by :

$$\nabla_{\rm ad} = \left(\frac{\partial \ln T}{\partial \ln P}\right)_{\rm s} \tag{2.6}$$

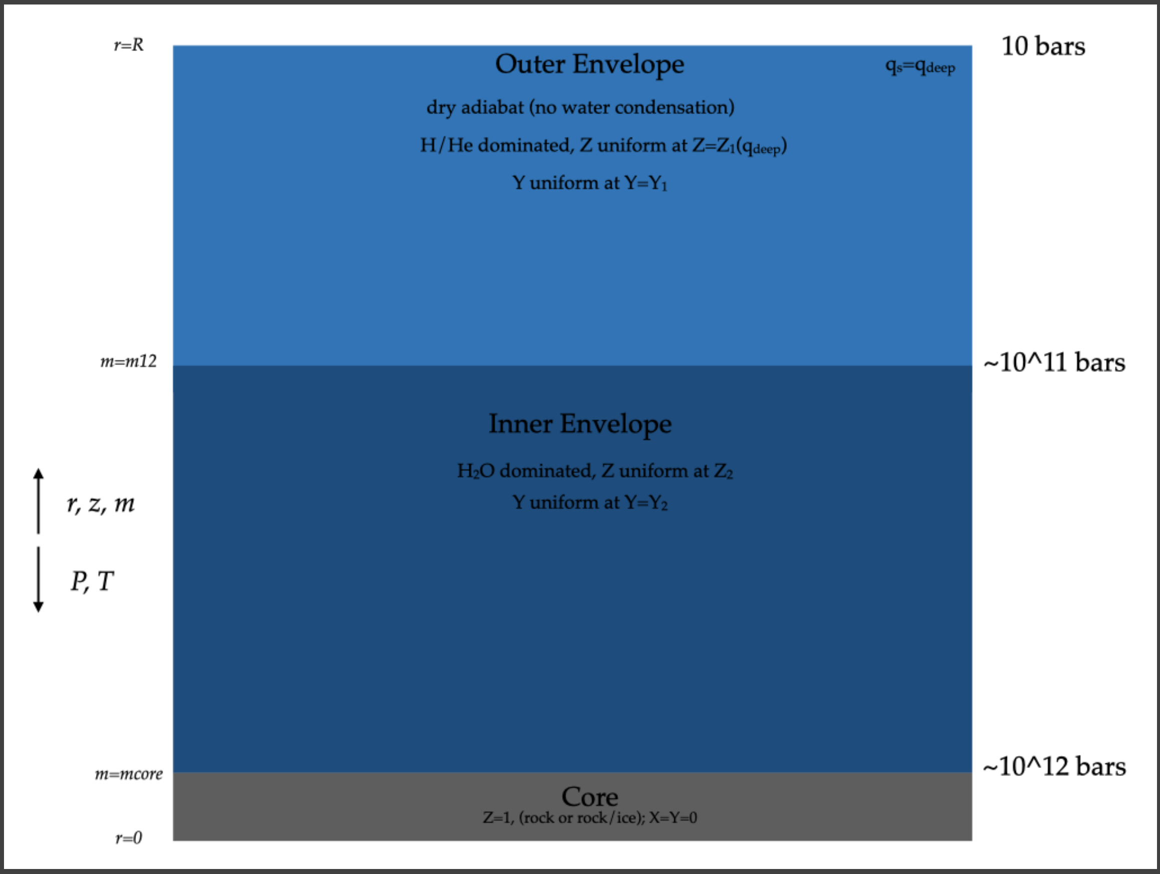

Figure 2.1: The structure for a fully convective, dry adiabatic interior. In this model, the inner and outer envelopes are assumed to be well mixed, fully convective, and following a dry adiabat. The core is composed of rock and ice. The inner envelope is water dominated, with with uniform concentrations of hydrogen, helium, and water; whereas, the outer envelope is hydrogen and helium dominated, with trace amounts of water. The 'atmosphere' exists above 10 bars.

Finally, beyond the outer envelope is the atmosphere. When modeling the thermal evolution of gas and ice giants, it has long been recognized that model atmospheres constitute an outer boundary condition for interior structure models, providing key inputs that impact cooling times for interior structure models. Our work considers both (Harold C. Graboske & Olness, 1975) and (Fortney et al., 2011) model atmospheres. Unless otherwise stated, our results will utilize the Fortney 2011 model atmospheres.

2.2 Inclusion of Moist Convection Within Outer Envelope

Our interior structure model departs from the standard model described above by adding a moist adiabatic layer to the outer envelope that, under favorable conditions, allows for the condensation of H_2O. Gases condense at at sufficiently low temperatures or high pressures(cite pierrehumbert). Condensation of a gas is characterized by its saturation vapor pressure, P_{sat}, given by:

$$P_{\text{sat}}(T) = P_{\text{sat}}(T_0)e^{-\frac{1}{R_{\text{gas}}}\left(\frac{1}{T}-\frac{1}{T_0}\right)} \tag{2.7}$$

where R_{gas} is the gas constant for the condensible species. When the partial pressure of a gas, P_{gas}, is less than P_{sat}, the parcel of gas is 'unsaturated'. When $P_{\text{gas}} = P_{\text{sat}}$, the gas is 'saturated'. And, when $P_{\text{gas}} > P_{\text{sat}}$, the parcel is 'supersaturated'. Each condensible species has its own saturation vapor pressure.

The condensation of water in the interior of hydrogen-dominated atmospheres has some notable differences with our experience of water condensation within our own planet's atmosphere (Leconte et al., 2017) (Friedson & Gonzales, 2017) (Guillot, 2019) (Guillot, 1995). On Earth, H_2O lighter than the background air, which is composed primarily of N_2. So, while condensation of water in the interiror of ice giants does release heat through the latent heat of condensation, which in the presence of a heavier background gas would result in an instability, the situation is different when the background is hydrogen-helium dominated. In this case, a strong vertical gradient in mean molecular weight arises, creating a negative buoyancy. This may result in the formation of a layer that is stable against convection (citations).

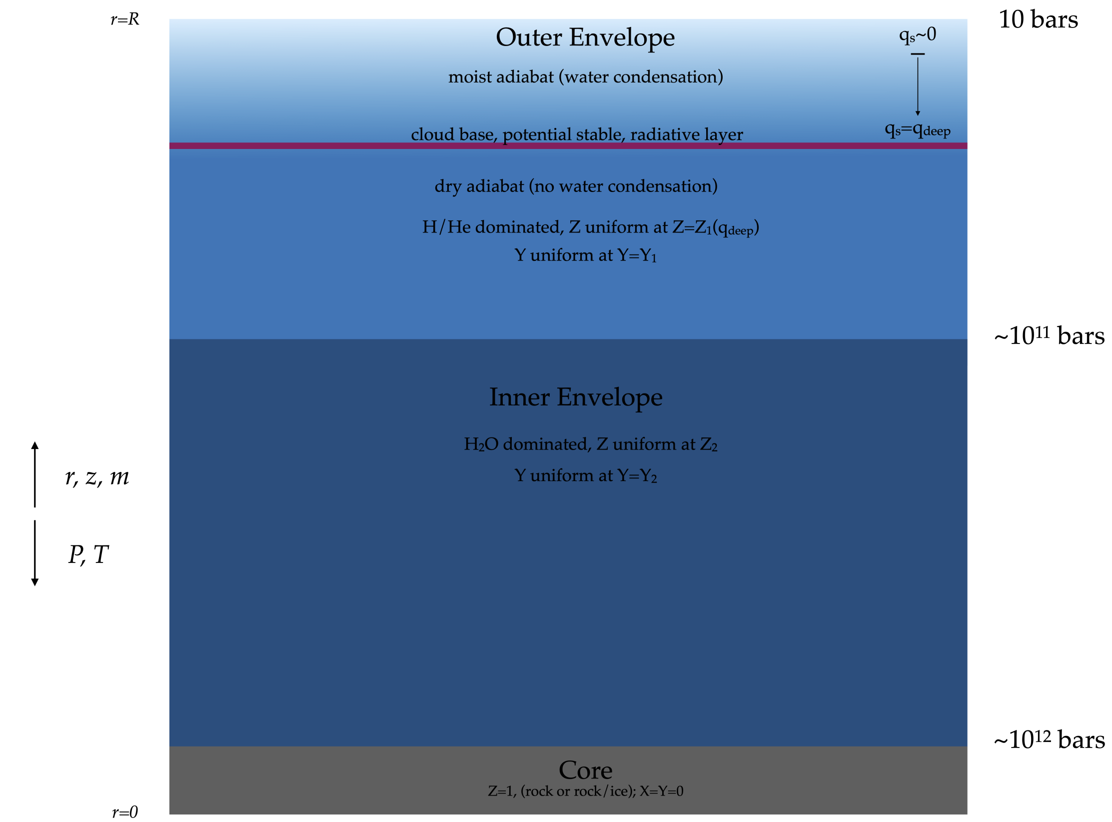

Figure 2.2: The structure for moist adiabatic interior, allowing for condensation-inhibited convection.

If condensation zone forms, it may be stable against convection. Convection is inhibited due to the formation of a stable condensation zone when $\alpha < 1$, where is α (Friedson & Gonzales, 2017) is given by:

$$\alpha = 1 + \xi(q_s L / R_W T_0) \tag{2.8}$$

If condensation is found to be inhibited,

At pressure where $\alpha < 1$, the cloud base of the water condensation zone forms. This thin, stable radiative layer has a temperature profile that is governed by:

$$T(P) = T_{\rm top} + \int_{P_{\rm top}}^{P} \left(\frac{dT}{dP}\right)_{\rm rad} dP \tag{2.9}$$

$$\left(\frac{dT}{dP}\right)_{\rm rad} = \frac{T}{P}\nabla_{\rm rad} = \frac{T}{P} \times \frac{3}{16}\frac{\kappa_R P}{g}\frac{T_{\rm int}^4}{T^4} \tag{2.10}$$

$$T_{\rm base} \equiv T(P + \Delta P) = T_{\rm top} + \left(\frac{dT}{dP}\right)_{\rm rad} \Delta P. \tag{2.11}$$

$$x_{\rm vap}(P, T) = x_{\rm vap}^{\rm sat}(P, T) = \frac{e_s(T)}{P}, \qquad P < P_{\rm base}. \tag{2.12}$$

$$x_{\rm vap}^{\rm sat}(P_{\rm base}, T_{\rm base}) = \frac{e_s(T_{\rm base})}{P_{\rm base}} = x_{\rm vap}^{\rm deep} \Longrightarrow \Delta P \equiv P_{\rm base} - P_{\rm top} = \frac{e_s(T_{\rm base})}{x_{\rm vap}^{\rm deep}} - P_{\rm top} \tag{2.13}$$

$$T_{\rm base} = T_{\rm top} + \left(\frac{dT}{dP}\right)_{\rm rad} \left(\frac{e_s(T_{\rm base})}{x_{\rm vap}^{\rm deep}} - P_{\rm top}\right) \tag{2.14}$$

Below the base of the radiative layer, the temperature-pressure profile again follows a dry adiabat, given by:

$$T(P > P_{\rm base}) = T_{\rm base} + \int_{P_{\rm base}}^{P} \left(\frac{dT}{dP}\right)_{\rm ad} dP \tag{2.15}$$

3

Results

3.1 Condensation-inhibited Convection

Talk about Figure 3.1.

3.2 Formation of Radiative Layer

Talk about Figure 3.2.

3.3 Thermal Evolution

Talk about Figure 3.3.

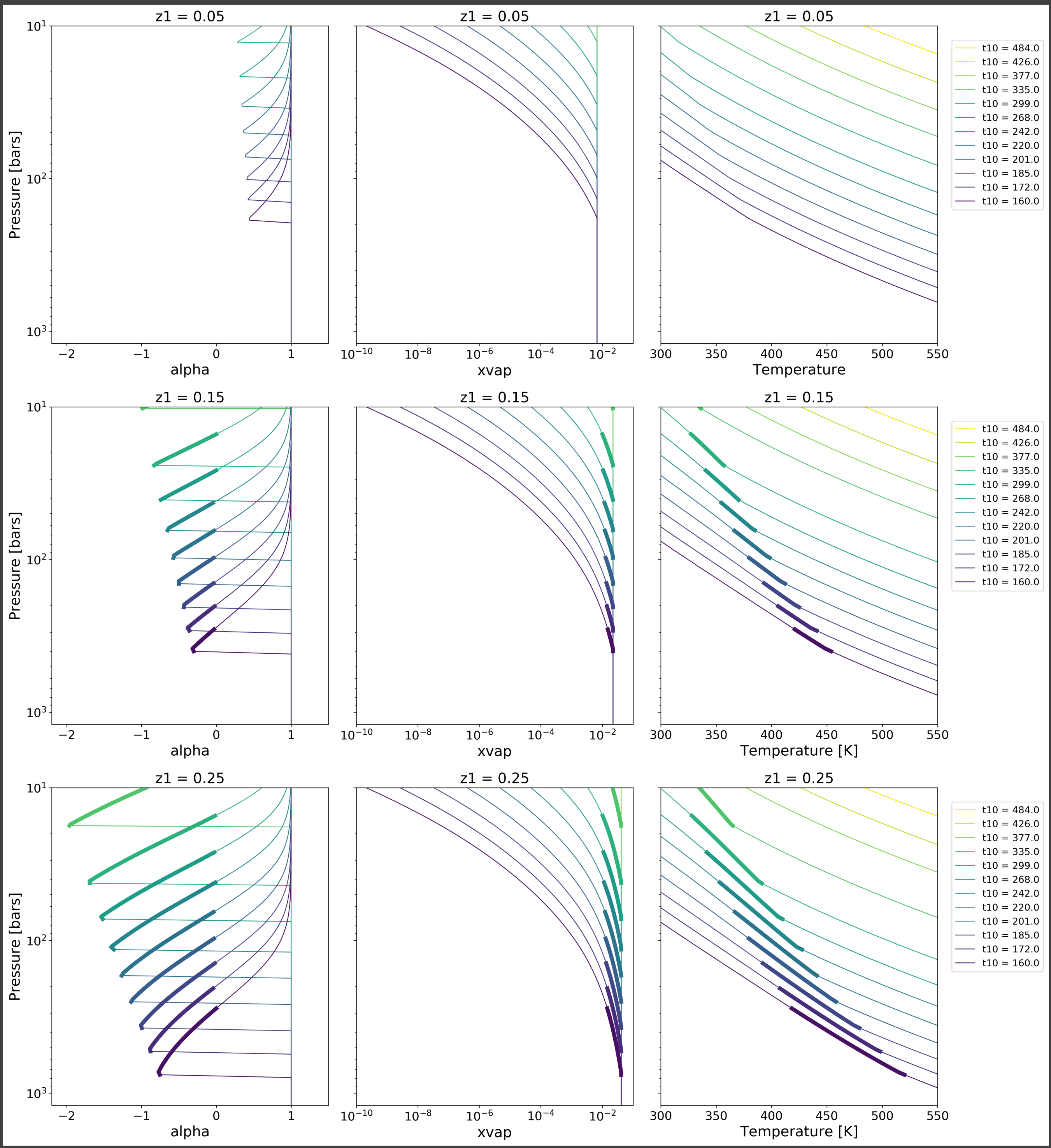

Figure 3.1: add description re: moist adiabat, when/where convection is inhibited and where the radiative zone base is in these plots. explain differences

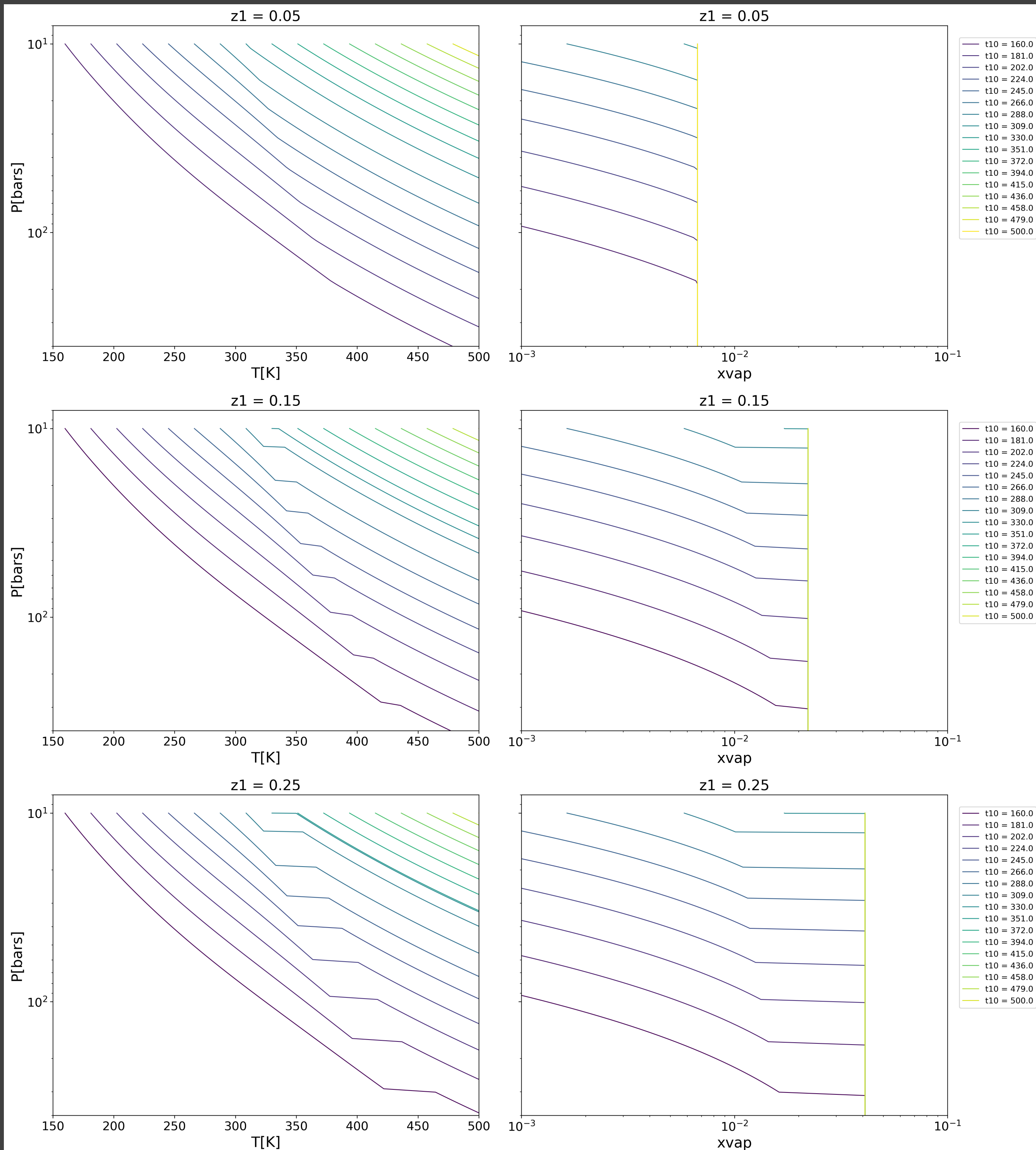

Figure 3.2: add description these plots. explain differences

4

Discussion and Conclusions

Appendix A

Some Ancillary Stuff

Bibliography

Fortney, J. J., Ikoma, M., Nettelmann, N., Guillot, T., & Marley, M. S. (2011). Self-consistent model atmospheres and the cooling of the solar system's giant planets. *The Astrophysical Journal*, 729, 32.

Friedson, A. J. & Gonzales, E. J. (2017). Inhibition of ordinary and diffusive convection in the water condensation zone of the ice giants and implications for their thermal evolution. *Icarus*, 297, 160–178.

Guillot, T. (1995). Condensation of methane, ammonia, and water and the inhibition of convection in giant planets. *Science*, (pp. 1697–1699).

Guillot, T. (2019). Uranus and neptune are key to understand planets with hydrogen atmospheres. *arXiv.org*.

Harold C. Graboske, Jr., J. B. P. A. S. G. & Olness, R. J. (1975). The structure and evolution of jupiter: The fluid contraction. *The Astrophysical Journal*, 199, 265–281.

Hubbard, W. (1977a). Comparative thermal evolution of uranus and neptune. *Icarus*, , 35, 177–181.

Hubbard, W. (1977b). The jovian surface condition and cooling rate. *Icarus*, , 30, 305–310.

L. Scheibe, N Nettelmann, R. R. (2019). Thermal evolution of uranus and neptune: Adiabatic models. *Astronomy and Astrophysics*, A70, 632.

Leconte, J., Selsis, F., Hersant, F., & Guillot, T. (2017). Condensation-inhibited convection in hydrogen-rich atmospheres: Stability against double-diffusive processes and thermal profiles for jupiter, saturn, uranus, and neptune. *Astronomy and Astrophysics*, A98, 598.

M. Podolak, W.B. Hubbard, D. S. (1991). Models of uranus' interior and magnetic field. *Uranus, Editors: J.T. Bergstralh, E.D. Miner, M. Shapely Matthews*, (pp.$\tilde{2}$9).

R. Kippenhahn, A. Weigert, A. W. (2012). *Stellar Structure and Evolution*. Springer.

S. Mazevet, A. Licari, G. C. & Potekhin, A. Y. (2019). Ab initio based equation of state of dense water for planetary and exoplanetary modeling. *Astronomy & Astrophysics*, A128, 621.

W.B. Hubbard, D. S. (1995). The interior of neptune. *Neptune and Triton, Editor: D.P. Kruikshank*, (pp. 109).

Y. Miguel, T. G. & Fayon, L. (2018). Jupiter internal structure: the effect of different equations of state. *Astronomy & Astrophysics*, C2, 618.